AD-A279 234 ON PAGE

...per response, including the time for reviewing instructions, searching existing data sources, gathering... ...collection of information. Send comments regarding this burden estimate or any other aspect of this ...Washington Headquarters Services, Directorate for Information Operations and Reports, 1215 Jefferson ...ement and Budget, Paperwork Reduction Project (0704-0188), Washington, DC 20503

1. AC...		6 May 94	3. REPORT TYPE AND DATES COVERED Technical 5/93–5/94

4. TITLE AND SUBTITLE
The Formulation of Quantum Statistical Mechanics Based on the Feynman Path Centroid Density IV. Algorithms for Centroid Molecular Dynamics

5. FUNDING NUMBERS
ONR N00014-92-J-1243

6. AUTHOR(S)
Jianshu Cao and Gregory A. Voth

DTIC
ELECTE
MAY 17 1994
S F D

7. PERFORMING ORGANIZATION NAME(S) AND ADDRESS(ES)

Department of Chemistry
University of Pennsylvania
Philadelphia, PA 19104-6323

8. PERFORMING ORGANIZATION REPORT NUMBER

ONR Technical Report #9

9. SPONSORING/MONITORING AGENCY NAME(S) AND ADDRESS(ES)

Office of Naval Research
Chemistry Division
800 North Quincy Street
Arlington, VA 22217-5000

10. SPONSORING/MONITORING AGENCY REPORT NUMBER

94-14659

11. SUPPLEMENTARY NOTES

12a. DISTRIBUTION/AVAILABILITY STATEMENT

Approved for public release: distribution unlimited

12b. DISTRIBUTION CODE

13. ABSTRACT *(Maximum 200 words)*

Numerical algorithms are developed for the centroid molecular dynamics (centroid MD) method to calculate dynamical time correlation functions for general many-body quantum systems. Approaches based on the normal mode path integral molecular dynamics and staging path integral Monte Carlo methods are described to carry out a direct calculation of the force on the centroid variables in the centroid MD algorithm. A more efficient, but approximate, scheme to compute the centroid force is devised which is based on the locally optimized harmonic approximation for the centroid potential. The centroid MD equations in the latter method can be solved with the help of an iterative procedure or through extended Lagrangian dynamics. A third algorithm introduces an effective centroid pseudopotential to approximate the full many-body centroid mean force potential by effective pairwise centroid interactions. Numerical simulations for both prototype models and more realistic many-body systems are performed to explore the feasibility and limitations of each algorithm.

14. SUBJECT TERMS

Chemical dynamics; computer simulation; electrochemistry

15. NUMBER OF PAGES
53

16. PRICE CODE

17. SECURITY CLASSIFICATION OF REPORT	18. SECURITY CLASSIFICATION OF THIS PAGE	19. SECURITY CLASSIFICATION OF ABSTRACT	20. LIMITATION OF ABSTRACT
Unclassified	Unclassified	Unclassified	

94 5 16 118

OFFICE OF NAVAL RESEARCH

GRANT N00014-92-J-1243

Technical Report No. 9

The Formulation of Quantum Statistical Mechanics Based on the Feynman Path Centroid Density. IV. Algorithms for Centroid Molecular Dynamics

by

Jianshu Cao and Gregory A. Voth

Submitted

to

Journal of Chemical Physics

University of Pennsylvania
Department of Chemistry
Philadelphia, PA 19104-6323

May 1994

TECHNICAL REPORT DISTRIBUTION LIST - GENERAL

Office of Naval Research (1)*
Chemistry Division, Code 313
800 North Quincy Street
Arlington, Virginia 22217-5000

Defense Technical Information
   Center (2)
Building 5, Cameron Station
Alexandria, VA 22314

Dr. James S. Murday (1)
Chemistry Division, Code 6100
Naval Research Laboratory
Washington, D.C. 20375-5000

Dr. Robert Green, Director (1)
Chemistry Division, Code 385
Naval Air Weapons Center
   Weapons Division
China Lake, CA 93555-6001

Dr. Elek Lindner (1)
Naval Command, Control and
   Ocean Surveillance Center
RDT&E Division
San Diego, CA 92152-5000

Dr. Richard W. Drisko (1)
Naval Civil Engineering
   Laboratory
Code L52
Port Hueneme, CA 93043

Dr. Harold H. Singerman (1)
Naval Surface Warfare Center
   Carderock Division Detachment
Annapolis, MD 21402-1198

Dr. Eugene C. Fischer (1)
Code 2840
Naval Surface Warfare Center
   Carderock Division Detachment
Annapolis, MD 21402-1198

Dr. Bernard E. Douda (1)
Crane Division
Naval Surface Warfare Center
Crane, Indiana 47522-5000

* Number of copies to forward

Accesion For	
NTIS CRA&I	☑
DTIC TAB	☐
Unannounced	☐
Justification	
By	
Distribution /	
Availability Codes	
Dist	Avail and / or Special
A-1	

The Formulation of Quantum Statistical Mechanics Based on the Feynman Path Centroid Density. IV. Algorithms for Centroid Molecular Dynamics

Jianshu Cao and Gregory A. Voth

Department of Chemistry, University of Pennsylvania, Philadelphia, Pennsylvania 19104-6323

Abstract

Numerical algorithms are developed for the centroid molecular dynamics (centroid MD) method to calculate dynamical time correlation functions for general many-body quantum systems. Approaches based on the normal mode path integral molecular dynamics and staging path integral Monte Carlo methods are described to carry out a direct calculation of the force on the centroid variables in the centroid MD algorithm. A more efficient, but approximate, scheme to compute the centroid force is devised which is based on the locally optimized harmonic approximation for the centroid potential. The centroid MD equations in the latter method can be solved with the help of an iterative procedure or through extended Lagrangian dynamics. A third algorithm introduces an effective centroid pseudopotential to approximate the full many-body centroid mean force potential by effective pairwise centroid interactions. Numerical simulations for both prototype models and more realistic many-body systems are performed to explore the feasibility and limitations of each algorithm.

I. INTRODUCTION

In a series of previous papers. [1-4] an intriguing perspective on quantum statistical mechanics has been extensively developed. This perspective involves the path centroid variable [5] in Feynman path integration. [6-12] (Hereafter. three of the preceding papers [2-4] will be referred to as Papers I. II. and III. respectively.) Perhaps the most interesting and promising result of the aforementioned research is an approximate method for computing quantum dynamical time correlation functions called "centroid molecular dynamics" (centroid MD). [1.3.4] The central concept of centroid MD was first introduced in Ref. [1] and then extensively analyzed and extended in Paper II. Paper III. which precedes the present paper. introduces a phase space centroid perspective and provides a definitive theoretical basis for centroid MD. Though a single one-dimensional quantum particle has largely served as the numerical example for centroid MD in the previous papers. [1,3,4] the method is by no means limited to such a simple prototype model. As a matter of fact, one prominent advantage of the method is the feasibility of its application to more complicated physical systems such as solvated quantum particles, high frequency vibrations of condensed phase polyatomic molecules. clusters and fluids consisting of quantum particles, and nonlinear quantum phonons. However. a central challenge is to first develop practical numerical algorithms for computing centroid MD in general many-body quantum systems. The present paper is devoted to this issue.

Before describing the algorithms for centroid MD, it is first necessary to briefly review the key developments in the earlier papers. In Paper I. the quasiclassical role for the path centroid variable and centroid density [5.13-15] in defining the *equilibrium* properties of quantum systems was fully elucidated. Then. building on the insights of an earlier communication. [1] the path centroid perspective was extended in Paper II to the realm of quantum *dynamics*. In that paper, a centroid-based perspective was uncovered for the calculation of quantum time correlation functions. A centroid time correlation function was introduced in those papers as an approximation for the Kubo transformed [16] position correlation func-

tion. The centroid correlation function is thus related to the usual quantum time correlation function through the Fourier transform relationship

$$\tilde{C}(\omega) = (\hbar\beta\omega/2)\left[\coth(\hbar\beta\omega/2) + 1\right]\tilde{C}^*(\omega) \quad . \tag{1.1}$$

where C^* denotes the centroid time correlation function. [1,3,4] It was argued that $C^*(t)$ should be computed from classical-like dynamics for the centroid variable on the mean centroid potential energy surface such that

$$C^*(t) = \langle q_c(t)q_c(0)\rangle_{\rho_c} \quad . \tag{1.2}$$

where $q_c(t)$ is the centroid trajectory for a given particle degree-of-freedom. The $3N$-dimensional centroid trajectories for a general system are generated by the effective classical equations of motion [1,3,4]

$$\mathbf{m} \cdot \frac{d^2}{dt^2}\vec{q}_c(t) = \vec{F}_c(\vec{q}_c) \quad , \tag{1.3}$$

where $\vec{q}_c(t)$ is the $3N$-dimensional column vector of centroid positions, $\mathbf{m}$ is the diagonal particle mass matrix, and $\vec{F}_c(\vec{q}_c)$ is the quantum mechanical centroid mean force vector. The latter quantity is expressed as the operation of a $3N$-dimensional gradient vector in centroid configuration space. $\vec{\nabla}_c$, on the mean centroid potential $V_c(\vec{q}_c)$, i.e..

$$\begin{aligned}
\vec{F}_c(\vec{q}_c) &= -\vec{\nabla}_c V_c(\vec{q}_c) \\
&= -\frac{\int \cdots \int \mathcal{D}\vec{q}(\tau)\,\delta(\vec{q}_c - \vec{q}_0)\left\{\vec{\nabla}V[\vec{q}(0)]\right\}\exp\left\{-S[\vec{q}(\tau)]/\hbar\right\}}{\int \cdots \int \mathcal{D}\vec{q}(\tau)\,\delta(\vec{q}_c - \vec{q}_0)\exp\left\{-S[\vec{q}(\tau)]/\hbar\right\}} \quad . \tag{1.4}
\end{aligned}$$

Here. $S[\vec{q}(\tau)]$ is the imaginary time action functional [6–9] and the imaginary time position centroid vector defined in Eq. (1.4) is

$$\vec{q}_0 = \frac{1}{\hbar\beta}\int_0^{\hbar\beta} d\tau\, \vec{q}(\tau) \quad . \tag{1.5}$$

The effective temperature-dependent centroid potential $V_c(\vec{q}_c)$ in Eq. (1.4) is defined by

$$V_c(\vec{q}_c) = -k_B T \ln\left\{\rho_c(\vec{q}_c)/[\prod_{i=1}^{N}(m_i/2\pi\hbar^2\beta)]^{3/2}\right\} \quad . \tag{1.6}$$

where the multidimensional position centroid density $\rho_c(\vec{q}_c)$ is given by [2.5]

$$\rho_c(\vec{q}_c) = \int \cdots \int \mathcal{D}\vec{q}(\tau)\, \delta(\vec{q}_c - \vec{q}_0)\, exp\left\{-S[\vec{q}(\tau)/\hbar]\right\} \quad . \tag{1.7}$$

In the centroid correlation function [Eq. (1.2)], the initial condition averaging denoted by $\langle \cdots \rangle_{\rho_c}$ is formally performed with the phase space version of Eq. (1.7) [1,3,4] in which the centroid momentum distribution simply factorizes into the *classical* Boltzmann momentum distribution.

In Paper III, the centroid formulation in multidimensional phase space allows one to prove that the centroid MD position correlation function is a well-defined approximation to the Kubo-transformed position correlation function. [4] The agreement between the two correlation functions can be demonstrated uniformly to all orders in a time expansion, with an error being proportional to the effective thermal width of the particle and the average anharmonicity of the mean centroid potential. The reader is referred to the preceding paper (Paper III) for an extensive discussion on this subject. In addition to this analytical justification, an earlier justification [1,3] was based on the analytic continuation of correlation functions obtained from the effective harmonic representation of the centroid density. [2.13-15] Moreover, centroid MD has been tested numerically for some non-trivial nonlinear systems and found to give excellent agreement with the exact result for the quantum position correlation function. [1,3] Several centroid MD strategies were also developed in Papers II and III to compute general quantum time correlation functions of the form $\langle A(t)B(0)\rangle$, where A and B are general quantum operators.

Although centroid MD appears to be a substantial breakthrough in the computation of (approximate) quantum time correlation functions, the determination of the centroid force in Eq. (1.3), as defined by Eq. (1.4), represents an algorithmic challenge for realistic many-body systems. Equation (1.4) shows that the centroid force is given by the average of the local potential gradient over quantum path fluctuations about the constrained centroid variables. Of course, all numerical path integral simulation techniques [17,18] can be adapted to compute this average, but the real issue is one of *computational efficiency* so that the

4

centroid force can be readily computed "on the fly" during the real time integration of the centroid MD equations [Eq. (1.3)]. This computation is not trivial for quantum many-body systems. (It is, however, clearly easier than a numerical "frontal assault" on the many-body time dependent Schrödinger equation or on real time Feynman path integrals. [6])

In the present paper, several algorithms will be developed and explored for the efficient computation of the centroid force in the centroid MD equations. Two of the approaches will be direct, or "brute force", numerical path integral approaches [17,18] in which the path averaging in Eq 1) is performed explicitly. These approaches will be based on a normal mode path integral MD algorithm [19] and·a staging path integral Monte Carlo (MC) algorithm. [20,21] with several numerical tricks introduced to speed up the computations. A rather different, and more efficient, direction will also be taken which approximates the centroid force within the framework of the locally optimized effective harmonic perspective. [2,13-15] The numerical details of solving the transcendental equations in the variational quadratic approximation are explored in some detail, and two independent algorithms are developed to optimize the variational parameters while simultaneously propagating the centroid MD variables in time. In addition, several schemes are proposed to simplify the evaluation of the Gaussian averages explicit in the variational theory. [2,13-15] Yet a third algorithm for centroid MD involves the calculation of the excess centroid free energy as a function of the separation between a pair of particles, representing this free energy by pairwise centroid pseudopotentials, and then running centroid MD simulations for an effective many-body system which interacts only through such pairwise interactions. The latter approximation reduces the full centroid mean potential hypersurface to the superposition of two-body centroid potentials and thus ignores static many-body quantum correlations. Nevertheless, the latter approach will provide a simple and effective alternative for centroid MD simulations of nearly classical or weakly interacting systems. All of the aforementioned algorithms are tested on several systems to demonstrate their overall feasibility and limitations.

The present paper is organized as follows: In Sec. II, two algorithms are described for the direct numerical calculation of the centroid force during a centroid MD simulation. Then.

5

in Sec. III an alternative and more numerically efficient method is explored which is based on the effective quadratic (i.e., approximate) theory for the centroid force. Several different aspects of the implementation of this algorithm are also discussed in some detail. Section IV then contains a description of the centroid pseudopotential method, while numerical implementations of all of the algorithms are presented in Sec. IV. Concluding remarks are given in Sec. V.

II. DIRECT CALCULATION OF THE CENTROID FORCE

In the discretized version of the Feynman path integral, [17,18] the centroid force in Eq. (1.4) is written as

$$F_c(q_c) = - \frac{\int \cdots \int \prod_{i=1}^{P} dq_i \, \delta(q_c - q_0) \, V'(q_1, \ldots, q_P) \, exp\left[-S_P(q_i, \ldots, q_P)/\hbar\right]}{\int \cdots \int \prod_{i=1}^{P} dq_i \, \delta(q_c - q_0) \, exp\left[-S_P(q_i, \ldots, q_P)/\hbar\right]} \quad . \qquad (2.1)$$

where, from the cyclic invariance of the trace,

$$V'(q_1, \ldots, q_P) \equiv \frac{1}{P} \sum_{i=1}^{P} \frac{dV(q)}{dq}\bigg|_{q=q_i} \qquad (2.2)$$

and the centroid variable in discrete notation is given by

$$q_0 = \frac{1}{P} \sum_{i=1}^{P} q_i \quad . \qquad (2.3)$$

The discretized path integral action functional is given by

$$S_P(q_i, \ldots, q_P) = \sum_{i=1}^{P} \left[\frac{mP}{2\hbar\beta} (q_{i+1} - q_i)^2 + \frac{\hbar\beta}{P} V(q_i) \right] \qquad (2.4)$$

Here, the discretization parameter is given by P and, for notational simplicity, the expressions are written for a single degree-of-freedom. An extension to many degrees-of-freedom is straightforward, although notationally more cumbersome.

In a path integral Monte Carlo (PIMC) calculation, the centroid force can be readily calculated from Eq. (2.1) by using the importance sampling function $exp[-S_P(q_i, \ldots, q_P)/\hbar]$ and pairwise MC moves to enforce the centroid constraint. For a path integral molecular

6

dynamics (PIMD) calculation. [22] one defines fictitious momenta p_i for each of the quasiparticles q_i and then runs an MD simulation with Hamilton's equations based on the fictitious Hamiltonian

$$H_P = \sum_{i=1}^{P} \frac{p_i^2}{2m'} + \sum_{i=1}^{P} \left[\frac{mP}{2\hbar^2\beta^2} (q_{i+1} - q_i)^2 - \frac{1}{P} V(q_i) \right] \quad . \qquad (2.5)$$

where. in the case of centroid MD. m' must equal m/P so that the centroid variable has the physical particle mass m. [1,3,4] If the PIMD trajectory adequately samples the canonical ensemble. then a particular time average over that trajectory will yield the centroid force. i.e.,

$$\begin{aligned} F_c(q_c) &= -\frac{1}{\hbar\beta} \int_0^{\hbar\beta} d\tau \langle V'[q(\tau)] \rangle_c \\ &= -\lim_{T\to\infty} \frac{1}{T} \int_0^T dt \, \frac{1}{P} \sum_{i=1}^{P} \frac{dV(q)}{dq} \bigg|_{q=q_i(t),q_0=q_c} \quad , \end{aligned} \qquad (2.6)$$

where $\langle \cdots \rangle_c$ denotes a centroid-constrained path integral average [cf. Eqs. (1.4) and (2.1)]. In a PIMD calculation, the centroid constraint must be enforced through, e.g., a holonomic constraint.

While a direct numerical path integral computation of the centroid force as outlined above will undoubtedly provide an accurate value of the centroid potential surface, the relevant question here is how to affect such a computation within the context of the time-integration of the centroid MD equations [Eq. (1.3)]. For low dimensional systems, the centroid force can indeed be first calculated for each point in space and stored on a grid in computer memory to be later recalled in the centroid MD calculation. As the dimensionality of the system increases. however, this straightforward procedure is no longer feasible due to the exponential growth of the required memory space. Consequently, for many-body systems one is forced to repeat a PIMD or PIMC calculation of the centroid force at each centroid MD time step (or over the interval of each time step). As it turns out, neither of the straightforward numerical path integral methods outlined above is feasible for this purpose. In the following two subsections. some more specialized algorithms for the calculation of the force in centroid MD are presented.

A. Normal Mode Path Integral Molecular Dynamics

One possible approach to the computation of the centroid force during a centroid MD calculation is based on the normal mode path integral molecular dynamics (NMPIMD) algorithm. Though NMPIMD has been discussed at length in a different context, [19] it will be presented here within the framework of centroid MD. In the NMPIMD algorithm, the centroid variable naturally separates from the other Feynman path modes. This feature provides an important simplification of the computation of the centroid force [Eq. (1.4)] and in distinguishing the sampling inherent in that computation from the real time propagation of the centroid variable. Moreover, the normal modes corresponding to the path fluctuations about the centroid can be assigned a smaller fictitious mass than the physical particle mass, leading to a more rapid convergence of the centroid force.

The basic idea of NMPIMD is to diagonalize some significant part of the Feynman action functional via a normal mode transformation, defined by

$$q_j \;=\; \sum_{n=1}^{P} a_n exp(-2\pi ijn/P) \tag{2.7}$$

where a_n is the normal mode coordinate. In order to shorten the computational time to perform the transformation in Eq. (2.7), one can take P to equal 2^k, where k is an integer, and then make use of the fast Fourier transform technique. By virtue of the orthonormality relation $\sum_{m=1}^{P} exp[2\pi im(l-n)/P] = P\delta_{nl}$, the above transformation will diagonalize any quadratic action functional. It should be noted that the normal mode propagator is different from the Fourier path integral (FPI) propagator [12,23] which is continuous in coordinate space but truncated in Fourier space. Unlike the convergence of the normal mode propagator which depends on the discretization parameter P, the convergence of the FPI propagator depends on the truncation parameter of the Fourier modes k_{max}.

Clearly, the computational effort implicit in NMPIMD relies on the efficiency of the path integral algorithm which, in turn, depends on the accuracy of the propagator used in the sampling. For example, it is advantageous to include the quadratic part of the potential

8

energy function in the definition of the NMPIMD propagator. The imaginary time action functional for a linear harmonic oscillator (LHO) is given in the discretized notation by

$$S_0(q_1, \ldots, q_P)/\hbar = \sum_{i=1}^{P} \frac{Pm}{2\hbar^2\beta} \frac{R}{sinh(R)} [(q_i^2 + q_{i-1}^2)cosh(R) - 2q_i q_{i-1}] \quad . \quad (2.8)$$

where $R = \hbar\beta\omega/P$, with ω being the LHO frequency. If the normal mode transformation in Eq. (2.7) is applied to this action, one obtains

$$S_0(a_1, \ldots, a_P)/\hbar = \sum_{n=1}^{P} \frac{|a_n|^2}{2\lambda_n^2}$$
$$= \sum_{n=1}^{(P/2)-1} \frac{(a_n^R)^2 + (a_n^I)^2}{\lambda_n^2} + \frac{(a_{P/2}^R)^2}{2\lambda_{P/2}^2} + \frac{(a_P^R)^2}{2\lambda_P^2} \quad . \quad (2.9)$$

where λ_n is the thermal width of the n-th normal mode, defined as

$$\lambda_n^2 = \frac{\lambda_\omega^2}{2P^2[1 - cos(2\pi n/P)] + b_\omega^2} \quad . \quad (2.10)$$

Here, the redefined parameters according to the exact LHO propagator in Eq. (2.8) are given by

$$\lambda_\omega^2 = \frac{\hbar^2\beta}{m} \frac{sinh(R)}{R} \quad (2.11)$$

and

$$b_\omega = \hbar\beta\omega \frac{sinh(R/2)}{(R/2)} \quad (2.12)$$

It is obvious from Eq. (2.9) that the Gaussian widths for the real part a_n^R and imaginary part a_n^I of the first $P/2 - 1$ modes are given by λ_n. On the other hand, $a_{P/2}$ and a_P are real variables with widths $\sqrt{2}\lambda_{P/2}$ and $\sqrt{2}\lambda_P$, respectively. The normal mode variables from $(P/2) + 1$ to $P - 1$ can be obtained by taking the complex conjugate of the first $(P/2) - 1$ variables according to the relation $a_n^* = a_{P-n}$.

From the above equations, it becomes apparent that the normal mode a_P in Eq. (2.9) is the centroid variable q_0 from Eq. (2.3) which is to be held constant during a NMPIMD calculation of the centroid force. One can therefore define an effective "Hamiltonian" for the remaining path modes by assigning them a set of fictitious momenta and masses, i.e.,

9

$$H_P(q_c) = \sum_{n=1}^{P-1}\left(\frac{|p_n|^2}{2m_n} + \frac{|a_n|^2}{2\beta\lambda_n^2}\right) + \frac{1}{P}\sum_{j=1}^{P}\Delta V(q_j) \qquad (2.13)$$

where p_n is the conjugate fictitious momentum for the normal mode a_n and ΔV is the residual potential, defined by

$$\Delta V(q) = V(q) - \frac{1}{2}m\omega^2(q - q_c)^2 \quad . \qquad (2.14)$$

Molecular dynamics can now by computed from Hamilton's equations based on this effective Hamiltonian, and the quasiparticle coordinates $\{q_j\}$ obtained as a function of time from Eq. (2.7). For the sake of efficiency, the fictitious masses are chosen as $m_n = m'/\beta\lambda_n^2$ so that all the normal modes oscillate with the same unit frequency. Otherwise, the NMPIMD time step will be determined by the timescale of the fast mode and the numerical integration of the slow modes becomes ineffective. To assure a canonical ensemble average over the normal modes, one can attach a Nose-Hoover chain to each of the mode variables. [24]

To our knowledge, this is the first attempt to implement a NMPIMD algorithm in any context. It should be noted that a very similar algorithm, called staging PIMD, [25] has already been implemented with considerable success for equilibrium path integral calculations. However, the NMPIMD algorithm is preferable for centroid MD calculations because the centroid variable is naturally identified from the normal mode transformation. Furthermore, the programming of NMPIMD is straightforward. A comment is in order, however, regarding the actual implementation of the NMPIMD centroid force algorithm for multidimensional systems. In such cases, the residual potential in Eq. (2.14) should be defined as the deviation of the exact potential from the quadratic potential which arises from *only* the diagonal elements of the Hessian matrix. The NMPIMD expressions given herein will thus basically be the same for each degree of freedom. Otherwise, a diagonalization of the Hessian matirx is first required at each centroid position in order to implement the NMPIMD algorithm as it has been presented. The numerical overhead inherent in such a diagonalization at every centroid MD time step is likely to be prohibitive within the context of the dynamical calculation. On the other hand, although the NMPIMD calculation of the centroid force

must eventually converge at each centroid position, the neglect of the off-diagonal terms of the Hessian matrix in the definition of the residual potential may slow the convergence. In such cases, NMPIMD can no longer be considered the method of choice for the computation of the centroid force and an alternative should be implemented (see the following sections).

The NMPIMD algorithm can be incorporated into a centroid MD calculation in two ways: The first is to calculate the centroid force using Eq. (2.6) at each time step in the centroid MD calculation. In this approach, the centroid force computation is algorithmically distinct from the centroid MD time integration. The second approach is to, in effect, compute the centroid force "on the fly" within the centroid MD algorithm. [26] This calculation can, in principle, be accomplished by making the fictitious masses $m_n = m'/\beta\lambda_n^2$ of the normal mode variables small enough so that the centroid force is convergently computed on the (longer) timescale of the centroid motion. In this case, the centroid force on that timescale is essentially given by

$$F_c(q_c) \simeq -\frac{1}{\Delta t_c} \int_0^{\Delta t_c} dt \; \frac{1}{P} \sum_{i=1}^{P} \frac{dV(q)}{dq}\bigg|_{q=q_i(t), q_0=q_c} . \tag{2.15}$$

where Δt_c is the time step needed to accurately integrate the slow centroid motion. Clearly, the average must converge on the timescale Δt_c. This algorithm is a kind of "extended Lagrangian" technique like the Car-Parrinello algorithm, [27,28] but there is an important difference. In the latter case, the goal is to have the parameters (e.g., plane wave coefficients) oscillate quickly and "tightly" around the minimum (i.e., the adiabatic ground state Born-Oppenheimer surface). In a centroid MD calculation, however, the idea is to have the path fluctuation modes sample their full *canonical equilibrium distribution* (and to do so quickly). Again, the canonical sampling can be facilitated by attaching a Nose-Hoover chain to each of the path fluctuation modes. [24]

Several other techniques can also be implemented to improve the convergence of the NMPIMD calculation of the centroid force in a centroid MD calculation. For example,

(a) The reference potential for defining the residual potential [Eq. (2.14)] can be updated at each time by setting the effective harmonic frequency [2.13-15] for the centroid force

calculation to be the frequency computed at the previous centroid time step, i.e.,

$$m\omega_c^2\big|_t = \langle V''\rangle_c\big|_{t-\Delta t_c} \quad .$$ (2.16)

The curvature of centroid potential can be evaluated along with the centroid force at any given centroid time step.

(b) If the reference potential is constantly optimized, the residual potential ΔV will be small and hence the MD motion of the normal modes will be dominated by the harmonic part. Therefore, a multiple time step procedure [29] seems most promising for such a calculation. In such a procedure, the linear motion of normal modes is integrated over a small time step, whereas the residual force is taken into account at much larger time intervals.

(c) In the case of an optimized reference potential, the effective anharmonicity of the residual potential should be small and the centroid force can be expanded linearly as

$$F_c(q_c') = F_c(q_c) + \frac{dF_c(q_c)}{dq_c}(q_c' - q_c)$$ (2.17)

where the centroid force gradient $dF_c(q_c)/dq_c$ is the curvature of the centroid mean potential, given by

$$\frac{dF_c(q_c)}{dq_c} = \frac{\partial^2 V_c(q)}{\partial q^2}$$

$$= \left\langle \frac{\partial^2 V}{\partial q^2}\right\rangle_c - \beta\left[\left\langle\left(\frac{1}{\hbar\beta}\int_0^{\hbar\beta} d\tau\, V'[q(\tau)]\right)^2\right\rangle_c - \left\langle\frac{1}{\hbar\beta}\int_0^{\hbar\beta} d\tau\, V'[q(\tau)]\right\rangle_c^2\right] \quad .$$ (2.18)

The imaginary time integrals in this expression can be readily expressed in discrete path integral notation [cf. Eq. (2.6)]. All the terms in Eq. (2.18) can then be evaluated along with the centroid force for a given centroid position. From Eq. (2.18), the deviation of the centroid force $F_c(q_c')$ at a new configuration q_c' from the exact centroid force $F_c(q_c)$ at the old configuration q_c can be assigned some tolerance, above which a new NMPIMD is initiated to calculate a new centroid force, etc., for the new configuration. In addition, the predicted centroid force $F_c(q_c')$ could also be compared to the classical force at q_c', the latter being used if the difference from the predicted centroid force falls below some tolerance.

The above list of numerical "tricks" is by no means exhaustive. There is a great deal of room for future algorithmic development in centroid MD.

12

B. Staging Path Integral Monte Carlo

As was pointed out earlier, the centroid force can be evaluated by either a PIMC or PIMD algorithm. A major drawback of the NMPIMD method is the consumptive computational effort involved in the normal mode transformation [Eq. (2.7)] at each time step to transform back to the quasiparticle coordinates. This transformation can become rather problematical if the number of path integral discretizations P is large. As an alternative, a centroid MD algorithm based on staging PIMC [20,21] is explored in the present subsection which is particularly advantageous if the number of discretizations is large.

The particular implementation of the staging algorithm in the present work follows closely the method discussed at length in Ref. [30]. However, it is helpful to first incorporate the effective harmonic reference system into the definition of the transition probability distribution function for selecting trial configurations of the path integral quasiparticle chain. [20,21,30] A LHO thermal propagator is given by

$$\rho_0(q, q', \tau) = \left(\frac{m}{2\pi\hbar^2\beta} \frac{R}{sinh(R)} \right)^{1/2} exp\left\{ -\frac{m}{2\hbar^2\beta} \frac{R}{sinh(R)} [(q^2 + q'^2)cosh(R) - 2qq'] \right\} \quad .$$

$$(2.19)$$

with $R = \hbar\omega\tau$. It can be shown that the transition probability function for a point q intermediate between two points q_1 and q_2 is given by

$$P(q) = \frac{\rho_0(q_1, q, \tau_1)\rho_0(q, q_2, \tau_2)}{\rho_0(q_1, q_2, \tau_1 + \tau_2)}$$

$$= \frac{1}{\sqrt{2\pi\lambda^2}} exp\left[-\frac{(q - q')^2}{2\lambda^2} \right] \quad .$$

$$(2.20)$$

where q' is the center of the Gaussian distribution, given by

$$q' = \frac{q_1 sinh(R_2) + q_2 sinh(R_1)}{sinh(R_1 + R_2)} \quad .$$

$$(2.21)$$

and λ is the width of the Gaussian distribution, given by

$$\frac{1}{\lambda^2} = \frac{m\omega}{\hbar} \left[\frac{1}{tanh(R_1)} + \frac{1}{tanh(R_2)} \right] \quad .$$

$$(2.22)$$

13

The above expressions can be reduced to the more standard free particle case [30] in the limit of $R \to 0$. In the context of the staging algorithm, Eq. (2.20) defines Levi's recursive scheme for directly sampling conditional Brownian motion paths which are then subjected to the acceptance probability, determined by the residual probability

$$\frac{\rho(q_1, q_2, \cdots, q_P)}{\rho_0(q_1, q_2, \cdots, q_P)} = exp\left[-\frac{\beta}{P}\sum_{i=1}^{P}\Delta V(q_i)\right] \quad . \tag{2.23}$$

where ΔV is given by Eq. (2.14).

An algorithmic challenge is to "smoothly" incorporate staging PIMD into the centroid MD time integration. An accurate centroid MD calculation may require a small enough time step so that the force difference in the numerical MD integrator becomes similar to the statistical error in the PIMC sampling of the centroid force. To deal with this issue, a single centroid MD time step Δt can be divided into N_{MC} segments. As a new MC chain configuration is sampled for a fixed centroid, the centroid can then be moved according to a much smaller time step $\delta t = \Delta t / N_{MC}$ using the force of the instantaneous MC path integral configuration. The N_{MC} staging PIMC samplings which are, in principle, to be performed at the beginning of each time step Δt, now become evenly distributed on a fine MD grid of spacing δt so that the PIMD evolves "on the fly" with the centroid MD motion. Such an approach should be more numerically effective than simply computing the centroid force at the beginning of each time step. Though the fluctuations of the centroid force can be observed on the fine timescale δt, the centroid trajectory becomes smooth on the larger timescale Δt. To some degree, this behavior is analogous to the stochastic motion of a heavy particle solvated in a light solvent, namely, Brownian motion. [31] The manifest diffusion of a Brownian particle consists of numerous collisions with light solvent particles. As the Brownian particle becomes heavier, the jigsaw behavior becomes less detectable. This is precisely the behavior of the centroid variable in centroid MD. In the extreme limit of $N_{MC} \to \infty$, one recovers the mean force average according to the PIMD case of $T \to \infty$ in Eq. (2.6). In this case, the force fluctuations on the centroid will become completely smoothed out so that the centroid feels the mean centroid MD force.

The complete staging PIMC centroid MD algorithm can be summarized as follows:

(1) Generate a MC chain segment (i.e.. moves of a subset of quasiparticles) by the staging method based on Eq. (2.20).

(2) Uniformly adjust the positions of all quasiparticles to fix the centroid position.

(3) Accept or reject the new configuration by comparing the change in the residual potential ΔV according to Eq. (2.23).

(4) Calculate the instantaneous centroid force for the resulting quasiparticle configuration and move the centroid accordingly for a small time step $\delta t = \Delta t / N_{MC}$ in the velocity Verlet algorithm.

(5) Repeat steps (1)–(4) N_{MC} times to complete one centroid MD time step Δt within the framework of the centroid MD integration.

The complete centroid MD simulation should to be carried out for different values of N_{MC} so that convergence of the the mean centroid force can be assured. Moreover, in the staging part of the algorithm [part (1)], the number of quasiparticles moved in each chain segment should be adjusted to achieve a reasonable MC acceptance ration in part (3). As in the NMPIMD method, the effective harmonic reference propagator in Eq. (2.19) for a multidimensional system can be defined from the diagonal terms of the Hessian matrix in order to avoid a costly diagonalization procedure.

C. General Considerations for the Direct Calculation of the Centroid Force

Clearly, the path integral average of the centroid force at each time step is the major workload of both path integral algorithms. Fortunately, the effort to sample the centroid force is much reduced in regions of low anharmonicity, for nearly classical systems. and/or for weakly interacting particles. This assertion can be demonstrated by explicitly expressing the centroid force fluctuations as

$$\delta f^2 \rangle_c = \frac{1}{3}\left[\left\langle \frac{\partial f}{\partial q}\right\rangle_c - \frac{\partial}{\partial q}\langle f\rangle_c\right] \simeq -\frac{1}{2\beta m}\frac{\partial C_c}{\partial \omega_c^2}\langle f''\rangle_c^2 \tag{2.24}$$

where $f(q) = V''(q)$. In the above equation, the first equality comes from the rearrangement of Eq. (2.18) and the second expression arises from the locally optimized effective harmonic approximation. [2.13–15] The resulting expression indicates that the quantum fluctuations of the centroid force are proportional to $\langle f'' \rangle_c^2$, which arises from the *averaged* anharmonicity of the potential, and from C_c which measures the effective quantum thermal dispersion of the particle. [2–4]

As a final point in this section, it is noted that in a direct path integral centroid MD calculation one can also explicitly compute the centroid-constrained path integral average of a quantum operator at each time t in the time integration (i.e., a Gaussian approximation for the averaged operator [3,4,32] can be avoided). Such averages are required in the method called "centroid MD with semiclassical operators" developed for the computation of the approximate centroid correlation function $C_{AB}^*(t)$ [cf. Eqs. (4.10) and (4.11) of Ref. [4]], so it is fortunate they can be obtained so directly.

III. EFFECTIVE HARMONIC COMPUTATION OF THE CENTROID FORCE

An alternative, highly efficient, algorithm for computing the centroid force in centroid MD makes use of the variational effective quadratic theory for the centroid potential. [1–4,13–15] This approach, which is approximate, represents the centroid potential as a locally optimized quadratic potential centered at the centroid position. The effective potential is then constantly updated as the centroid propagates in the MD time evolution.

Following the multidimensional formalism presented in Paper III, an effective quadratic centroid force constant matrix can be introduced as

$$
\begin{aligned}
\mathbf{K}_c(\vec{q}_c) &= \langle \mathbf{K}(\vec{q}_c + \vec{\bar{q}}) \rangle_c \\
&= \frac{1}{\sqrt{\det[2\pi \mathbf{C}_c(0, \vec{q}_c)]}} \int d\vec{\bar{q}} \, \mathbf{K}(\vec{q}_c + \vec{\bar{q}}) \, exp\left[-\vec{\bar{q}} \cdot \mathbf{C}_c^{-1}(0, \vec{q}_c) \cdot \vec{\bar{q}}/2 \right]
\end{aligned} \tag{3.1}
$$

where the Gaussian width factor matrix $\mathbf{C}_c(0, \vec{q}_c)$, in this case, is the position sub-block of the generalized centroid-constrained correlation function matrix in Eq. (2.5) of Paper III.

16

The Hessian matrix in Eq. (3.1) is defined by

$$[\mathbf{K}(\vec{q})]_{ij} = \frac{\partial^2 V(\vec{q})}{\partial q_i \partial q_j} \quad . \tag{3.2}$$

On the level of the effective quadratic approximation. the Gaussian width matrix is formally expressed as,

$$\mathbf{C}_c(0, \vec{q}_c) = \sum_{n \neq 0} \left[\beta \mathbf{m} \Omega_n^2 + \beta \mathbf{K}_c(\vec{q}_c) \right]^{-1} \quad . \tag{3.3}$$

where $\mathbf{m}$ is the $3N$−dimensional particle mass matrix and $\Omega_n = 2\pi n / \hbar \beta$. A centroid-dependent unitary matrix $\mathbf{U}(\vec{q}_c)$ can be found to diagonalize the mass-scaled centroid force constant matrix $\overline{\mathbf{K}}_c(\vec{q}_c)$, giving the eigenfrequencies

$$\mathbf{U}^\dagger(\vec{q}_c) \, \overline{\mathbf{K}}_c(\vec{q}_c) \, \mathbf{U}(\vec{q}_c) = \mathbf{I} \cdot \vec{\omega}_c^2 \quad . \tag{3.4}$$

where $\vec{\omega}_c^2$ is the column vector of centroid-dependent eigenvalues and $\mathbf{I}$ is the $3N$−dimensional identity matrix. The Gaussian width factor matrix in Eq. (3.1) can be determined from the relation

$$\mathbf{C}_c(0, \vec{q}_c) = \overline{\mathbf{U}}(\vec{q}_c) \left[\mathbf{I} \cdot \vec{\bar{\alpha}}(\vec{q}_c) \right] \overline{\mathbf{U}}^\dagger(\vec{q}_c) \quad , \tag{3.5}$$

where the individual elements of the normal mode thermal width factor vector are given by

$$\bar{\alpha}_l(\vec{q}_c) = \frac{1}{\beta \omega_{c,l}^2} \left\{ \frac{(\hbar \beta \omega_{c,l}/2)}{tanh(\hbar \beta \omega_{c,l}/2)} - 1 \right\} \tag{3.6}$$

and the mass-scaled unitary matrix $\overline{U}(\vec{q}_c)$ is given by

$$\overline{\mathbf{U}}(\vec{q}_c) = \mathbf{m}^{-1/2} \mathbf{U}(\vec{q}_c) \quad . \tag{3.7}$$

Thus, the set of optimized frequencies $\{\omega_{c,l}\}$ are variationally obtained as the self-consistent solution to the transcendental matrix equations (3.1)−(3.8) for a given centroid position.

A. Evaluation of the Gaussian Averages

A central algorithmic challenge in using the effective harmonic theory is the computation of the Gaussian averages inherent in the variational expression for the centroid potential. [2-4.13-15] The latter expression is given by

17

$$\langle V(\vec{q}_c + \vec{\bar{q}})\rangle_c \; = \; \frac{1}{\sqrt{\det[2\pi \mathbf{C}_c(0,\vec{q}_c)]}} \int d\vec{\bar{q}} \; V(\vec{q}_c + \vec{\bar{q}}) \, exp\left[-\vec{\bar{q}} \cdot \mathbf{C}_c^{-1}(0,\vec{q}_c) \cdot \vec{\bar{q}}/2\right] \quad . \qquad (3.8)$$

From this expression. one can obtain the effective harmonic approximation to the centroid force. given by

$$\vec{F}(\vec{q}_c) \; = \; -\vec{\nabla}_c \langle V(\vec{q}_c + \vec{\bar{q}})\rangle_c \Big|_{\mathbf{C}_c} \quad . \qquad (3.9)$$

where the notation "$\cdots|_{\mathbf{C}_c}$" indicates that the centroid derivatives in the gradient do not act on the width matrix $\mathbf{C}_c$. The elements of the centroid-dependent force constant matrix in Eq. (3.1) can be similarly expressed as

$$[\mathbf{K}_c(\vec{q}_c)]_{ij} \; = \; \frac{\partial^2}{\partial q_i \partial q_j} \langle V(\vec{q}_c + \vec{\bar{q}})\rangle_c|_{\mathbf{C}_c}. \qquad (3.10)$$

It should be pointed out that the Gaussian-averaged potential at the centroid $\vec{q}_c$ in Eq. (3.8) is different from the effective centroid potential introduced in Eq. (1.6). However, the centroid force in Eq. (3.9) can be shown to be the effective harmonic approximation to the exact centroid force in Eq. (1.4).

Many systems can be well described by pairwise (or site-site) potentials. If such is the case. the Gaussian average in Eq. (3.8) can be expressed in terms of the summation over all pair interactions. i.e..

$$\langle V(\vec{q}_c + \vec{\bar{q}})\rangle_c \; = \; \sum_{i=1}^{N}\sum_{j>i}^{N} \langle v(\vec{r}_{ij})\rangle_c \quad . \qquad (3.11)$$

where $\vec{r}_{ij}$ is the three-dimensional vector connecting the i-th and j-th particles. For a specific pair of interactions. the other degrees of freedom can be integrated out of the average, leading to a Gaussian average in a lower-dimensional space:

$$\langle v(\vec{r}_{ij})\rangle_c \; = \; \frac{1}{\sqrt{\det[2\pi \mathbf{C}'_{c,ij}(\vec{q}_c)]}} \int d\vec{\bar{r}} \; v(\vec{r}_{c,ij} + \vec{\bar{r}}) \, exp\left[-\vec{\bar{r}} \cdot \mathbf{C}'^{-1}_{c,ij}(\vec{q}_c) \cdot \vec{\bar{r}}/2\right] \quad . \qquad (3.12)$$

where the 3-dimensional. centroid-dependent submatrix $\mathbf{C}'_{c,ij}(\vec{q}_c)$ can be reduced from the full matrix width factor $\mathbf{C}_{c,ij}(0,\vec{q}_c)$. The expression for $\mathbf{C}'_{c,ij}(\vec{q}_c)$ and its derivation can be found in the Appendix. The above simplification reduces the computational effort considerably for

systems described by pair potentials. It must be noted. however. that the submatrix $C'_{c,ij}(\vec{q}_c)$ still depends on the global configuration of the particle centroids. In practice. however. it can be assumed that the effective widths of a pair of particles will not be affected by a change in the position of those particles if they are beyond some cut-off separation.

The Gaussian average in Eq. (3.8) can only be carried out analytically for polynomials. Gaussian potentials. exponentials. and their combinations. Gaussian averages of other functions cannot be expressed in closed analytical forms. The numerical integration of even a three-dimensional Gaussian average [cf. Eq. (3.12) is time consuming and would reduce the efficiency of the effective harmonic algorithm for centroid MD. These difficulties are magnified when several iterations are required to achieve a convergent solution to the variational transcendental equations. The best strategy therefore, is to represent the physical potential by a set of functions which can be Gaussian averaged analytically. Several such approaches are discussed below which may be appropriate under different circumstances.

1. Taylor Series Expansion

In the nearly classical regime. the Gaussian width matrix. i.e.. the centroid-constrained propagator matrix $C_c(0, \vec{q}_c)$, is a small quantity so the Taylor expansion of the force constant matrix $K(\vec{q}_c + \vec{\vec{q}})$ in Eq. (3.1) can be truncated at the first nonvanishing term. giving

$$K_c(\vec{q}_c) \simeq K(q_c) + \frac{1}{2}C_c(0, \vec{q}_c) : [\partial_i\partial_j K(\vec{q}_c)] \quad . \tag{3.13}$$

where $\partial_i\partial_j K(\vec{q}_c)$ is a fourth-order tensor. The centroid force expression is of a similar form. but with the matrices K_c and K replaced by the vectors $\vec{F}_c$ and $\vec{F}$. respectively. For pairwise interactions. the force constant expression can be reduced to one in three-dimensions with C'_c replacing C_c in Eq. (3.13).

2. Gaussian Fit of the Potential

Few physical potentials resemble a Gaussian function. However. by least-squares fitting the potential data. Gaussian functions can be used to represent any physical potential. i.e..

$$V(\vec{q}) = \sum_{l=1}^{N_l} \gamma_l \, exp\left[-(\vec{q}-\vec{d_l}) \cdot \mathbf{A}_l^{-1} \cdot (\vec{q}-\vec{d_l})/2\right] \quad . \tag{3.14}$$

where $\mathbf{A}_l$ is the Gaussian width matrix for a given index l. Since the set of Gaussians does not rigorously form a complete set. Eq. (3.14) is not an expansion but is instead an approximate fitting of representative points in the range important for the particle interactions.

With the above expression in hand. one can easily complete the Gaussian integration in Eq. (3.8). giving explicitly

$$\langle V(\vec{q_c}+\vec{q})\rangle_c = \sum_{l=1}^{N_l} \frac{\gamma_l}{\det(\mathbf{A}_l^{-1}\mathbf{C}_c+1)} \, exp\left[-(\vec{q_c}-\vec{d_l}) \cdot (\mathbf{A}_l+\mathbf{C}_c)^{-1} \cdot (\vec{q_c}-\vec{d_l})/2\right] \tag{3.15}$$

which indicates that the Gaussian averaging broadens the original Gaussian fitting width. If the interaction is described by a pairwise central force. the Gaussian average can be carried out for each pair in Eq. (3.11), giving

$$\langle v(\vec{r}_{ij})\rangle_c = \sum_{l=1}^{N_l} \frac{\gamma_l}{\det(\mathbf{a}_l^{-1}\mathbf{C}_c'+1)} \, exp\left[-\vec{r}_{c,ij} \cdot (\mathbf{a}_l+\mathbf{C}_c')^{-1} \cdot \vec{r}_{c,ij}/2\right] \quad . \tag{3.16}$$

Here. $\mathbf{a}_l = a_l\mathbf{I}$. where a_l is a constant for a pair potential. In particular. the pair potential between two sites is fit by Gaussians as

$$v(r) = \sum_{l=1}^{N_l} \gamma_l \, e^{-r^2/2a_l} \quad . \tag{3.17}$$

This expression represents the simplest possible Gaussian fit in which the origin of each Gaussian is taken to be $r = 0$. The fitting procedure can obviously be generalized to use distributed Gaussians.

3. Hermite Polynomial Representation of Pair Potentials

In principle. any pair potential can be rigorously expanded in terms of the complete set of eigenfunctions of the linear harmonic oscillator. These functions are the product of

20

Hermite polynomials and a Gaussian function. Thereby, the Gaussian averages of those basis functions in Eq. (3.8) can be written as combinations of Gaussian functions, polynomials, and error functions. This approach, because of its rigor, has an advantage over the previous two approximations. However, it will be more complicated both analytically and numerically. The details of this approach will be left for future investigations.

4. Plane Wave Representation of Pair Potentials

A given pairwise interaction between particles or molecular sites can also be expanded in terms of a discrete set of planewaves. In this case, the pair terms in Eq. (3.11) can be expressed as

$$v(\vec{r}_{ij}) \; = \; \sum_{\vec{k}} \hat{V}_{\vec{k}} \, exp(i\vec{k} \cdot \vec{r}_{ij}) \quad . \tag{3.18}$$

where $\hat{V}_{\vec{k}}$ is the three-dimensional Fourier transform of the pair potential for the discrete wavevector $\vec{k}$. After performing the Gaussian averaging explicit in Eq. (3.12), one obtains for the terms in Eq. (3.11) the expression

$$\langle v(\vec{r}_{ij}) \rangle_c \; = \; \sum_{\vec{k}} \hat{V}_{\vec{k}} \, exp\left[i\vec{k} \cdot \vec{r}_{c,ij} \, - \, \vec{k} \cdot C_c'(\vec{q_c}) \cdot \vec{k}/2 \right]. \tag{3.19}$$

This approach is both mathematically rigorous and simple to implement, but it can become computationally expensive if a large number of planewave basis functions are required to fit the pair potential.

Having discussed strategies for computing the Gaussian averages explicit in the effective harmonic theory, two algorithms will now be described for carrying out centroid MD calculations using the effective harmonic representation of the centroid force.

B. An Extended Lagrangian Method

The optimal parameters for the effective harmonic approximation to the centroid potential $V_c(\vec{q_c})$ [Eq. (1.6)] are determined by a variational minimization of $V_c(\vec{q_c})$ with respect

21

to those parameters. [2.13-15] This minimization is accomplished with the help of a Gibbs-Bogoliubov variational principle for the centroid potential (i.e.. centroid free energy). [33] Therefore. an extended Lagrangian technique [27.28] can be employed to minimize the effective centroid potential and the resulting centroid force while simultaneously propagating the centroid variables in time. The similarity between centroid MD with the effective harmonic theory for the centroid force and the Car-Parrinello (CP) extended Lagrangian method [27.28] is clear: The centroid motion is the analogue to the CP nuclear motion. the variational parameters in the effective harmonic theory are the analogues to the CP planewave coefficients. and the centroid potential is similar to the ground state CP adiabatic energy functional. In order to outline the extended Lagrangian method as it applies to centroid MD. the following discussion will be restricted to a one-dimensional problem for simplicity. The algorithm for multidimensional systems is described at the end of the section.

In the effective harmonic approximation. [2,13-15] the centroid potential in Eq. (1.6) is given by

$$V_c(q_c; \xi) = -k_B T \, ln[(b/2)/\sinh(b/2)] + \langle V(q_c + \bar{q}) \rangle_c - m\omega_c^2 C_c(0, q_c)/2 \quad . \qquad (3.20)$$

where $b = \hbar \beta \omega_c$, with ω_c being the frequency of the effective harmonic potential. and the effective harmonic expression for $C_c(0, q_c)$ is given in Eq. (3.3). The parameter ξ is the variational parameter which is optimized to minimize the centroid potential. The parameter can be chosen to be the centroid frequency ω_c or the width factor C_c.

At this point. one can introduce the extended Lagrangian

$$L_{ex}(\dot{q}_c, \dot{\xi}, q_c, \xi) = \frac{1}{2} m \dot{q}_c^2 + \frac{1}{2} m_\xi \dot{\xi}^2 - V_c(q_c; \xi) \quad . \qquad (3.21)$$

where $\dot{\xi}$ is the velocity associated with the variational parameter ξ. and m_ξ is its fictitious mass. The above Lagrangian forms the basis for the centroid MD equations in which the variational parameter ξ and. in turn. the centroid force are computed simultaneously with the centroid motion.

If the variational parameter ξ is taken to be the frequency ω_c. one obtains the nonlinear equation for the fictitious force on that variable. i.e..

$$F_{\omega_c}(q_c, \omega_c) \equiv -\frac{\partial V_c(q_c; \omega_c)}{\partial \omega_c}$$

$$= -\frac{\hbar g(b)}{m\omega_c^2}\left[\langle \partial_c^2 V(q_c + \tilde{q})\rangle_c - m\omega_c^2\right] \qquad (3.22)$$

where ∂_c is the partial derivative with respect to the centroid variable, and

$$g(b) = \frac{1}{b} - \frac{1}{4\tanh(b/2)} - \frac{b}{8\sinh^2(b/2)} \qquad . \qquad (3.23)$$

The centroid constrained average in Eq. (3.22), which depends on ω_c, is given from Eq. (3.1). The variational solution for the optimized centroid free energy [2,13–15] can obtained by setting Eq. (3.22) equal to zero and self-consistently solving for the variational parameter ω_c at a given centroid position. This variational solution provides the initial condition for the ξ trajectory generated by the Euler-Lagrange equations based on the extended Lagrangian [Eq. (3.21)].

If the variable ξ in the extended Lagrangian is instead taken to be the Gaussian width factor C_c, one obtains the fictitious force

$$F_{C_c}(q_c, C_c) \equiv -\frac{\partial V_c(q_c; C_c)}{\partial C_c}$$

$$= -\frac{1}{2}\left[\langle \partial_c^2 V(q_c + \tilde{q})\rangle_c - m\omega_c^2\right] \qquad (3.24)$$

in which the following relation has been used:

$$\frac{\partial C_c}{\partial \omega_c^2} = \frac{\hbar}{m\omega_c^3} g(b) \qquad . \qquad (3.25)$$

Since the width factor C_c is in this case the dynamical variable instead of ω_c, the centroid frequency can be obtained from C_c through the one-dimensional versions of Eqs. (3.5) and (3.6). As in the case of $\xi = \omega_c$, the optimal variational value for C_c is obtained by setting Eq. (3.24) equal to zero and self-consistently solving for C_c. For a given centroid initial condition, this value of C_c would provide the initial condition for the variable C_c in the extended Lagrangian simulation.

Though the choice of the variational parameter ξ in Eq. (3.21) is equivalent for the minimization of the centroid free energy, Eq. (3.24) is much easier to generalize to multidimensional systems, giving

$$-\frac{\partial V_c(\vec{q_c}; \mathbf{C}_c)}{\partial \mathbf{C}_c} = -\frac{1}{2}\left[\mathbf{K}_c(\vec{q_c}) - \overline{\mathbf{U}}(\vec{q_c})\,\mathbf{I} \cdot \overrightarrow{\omega_c^2}\, \overline{\mathbf{U}}^{\,\tau}(\vec{q_c}) \right] \tag{3.26}$$

where the relevant quantities here are defined in Eqs. (3.1)–(3.8). For a system of $3N$ degrees of freedom. there are $3N(3N+1)/2$ independent variational variables (i.e.. elements of the matrix $\mathbf{C}_c$). The multidimensional trajectory from the extended Lagrangian generates the width factor matrix $\mathbf{C}_c(t)$ as a function of time. In order to compute the force in Eq. (3.26), the matrix trajectory $\mathbf{C}_c(t)$ is used in Eq. (3.1) to compute the first term on the right-hand-side of Eq. (3.26). The second term is extracted from $\mathbf{C}_c(t)$ by inverting Eq. (3.5) to get the elements $\alpha_l(\vec{q_c})$ and. in turn, by solving for the vector $\overrightarrow{\omega_c^2}$ from Eq. (3.6). The latter vector. along with the transformation matrix $\overline{\mathbf{U}}(\vec{q_c})$, is then used in the second term on the right-hand-side of Eq. (3.26).

The essence of the extended Lagrangian method [27,28] is to choose such small fictitious masses $\{m_\xi\}$ in the multidimensional version of Eq. (3.21) that the fictitious variables $\{\xi\}$ rapidly oscillate around the minimum of the centroid free energy surface Eq. (3.20). The centroid variables should then exhibit an adiabatic, conservative motion because there is little energy exchange between them and the fictitious degrees of freedom. One useful technique is to associate a Nose-Hoover chain [24] to each fictitious variable to keep it from heating up.

C. An Iterative Method for the Centroid Force

While the extended Lagrangian method discussed above is quite elegant. it turns out that a simple iterative solution is quite feasible for the multidimensional effective harmonic variational equations [i.e.. Eq. (3.26) set equal to zero]. This algorithm is rather straight-forward: Solve the transcendental equation iteratively at a fixed centroid until convergence. calculate the centroid force and move the centroid accordingly in the MD integrator. and repeat the procedure for each time step. Many fewer iterations are required if the optimal parameters from the previous time step are used as the initial guess at the current time step.

Provided the centroid displacement is small, the convergence of the iterative scheme should be fast.

One difficulty associated with the iterative method occurs when negative curvatures are present in the classical Hessian matrix for a given centroid configuration (i.e., at inflection points or in a barrier region). If the initial guess of parameters is poor, the iterative scheme may not converge, even though the Gibbs-Bogoliubov variational principle [33] insures the centroid potential is finite and therefore that a solution must exist. If such a problem arises in the convergence of the iterative algorithm at a given time step, the iterative process can be re-started with a smaller value of $\hbar$ and that parameter can then be adjusted until the neighborhood of a fixed point is located. For $\hbar = 0$, the classical force is obtained which, of course, is well-defined. It should be noted that the effective quadratic theory is being implemented here within the context of the *local* centroid force for each time step in the centroid MD integration. This local instantaneous centroid potential is *not* being used to extrapolate the dynamics to long times. If such were the case, unphysical instabilities in the centroid dynamics might indeed be present.

IV. A PSEUDOPOTENTIAL METHOD FOR THE CENTROID FORCE

For a system consisting of particles interacting through pairwise potentials, the three-body quantum correlations will diminish as the distances increase. Therefore, at relatively dilute densities only the pairwise interactions need to be treated quantum mechanically. This approximation in the centroid theory is analogous to a treatment of many-body electronic polarization interactions through only a pairwise London-like attraction force, thus neglecting the higher-order many-body dispersion terms. The analogy in this case is drawn between the quantum path fluctuations about the particle centroids and the electronic fluctuations about the mean particle wavefunctions. The latter many-body dispersion problem has been systematically studied [34] through a quantum Drude oscillator model [35] and it was found that at low densities the two-body interaction is by far the dominant one.

The exact excess free energy of the centroids of a many body system can be approximated as the superposition of the excess free energy of the pair centroid interactions. i.e..

$$V_c(\vec{q}_c) \simeq \sum_{i=1}^{N} \sum_{j>i}^{N} v_{eff}(r_{c,ij}) \quad .$$ (4.1)

where the effective centroid pair potential $v_{eff}(r_{c,ij})$ is computed from the expression for two particles:

$$exp[-\beta v_{eff}(r_{c,12})]$$
$$= \frac{\int \cdots \int \mathcal{D}\vec{q}_1(\tau)\mathcal{D}\vec{q}_2(\tau)\,\delta(r_{c,12} - \tilde{r}_{12})\,exp\{-S[\vec{q}_1(\tau),\vec{q}_2(\tau)]/\hbar\}}{\int \cdots \int \mathcal{D}\vec{q}_1(\tau)\mathcal{D}\vec{q}_2(\tau)\,\delta(r_{c,12} - \tilde{r}_{12})\,exp\{-S_{fp}[\vec{q}_1(\tau),\vec{q}_2(\tau)]/\hbar\}} \quad .$$ (4.2)

Here. $\vec{q}_1$ and $\vec{q}_2$ are the three-dimensional vectors for particles "1" and "2". respectively. $S[\vec{q}_1(\tau),\vec{q}_2(\tau)]$ is the action functional for the interacting particles. $S_{fp}[\vec{q}_1(\tau),\vec{q}_2(\tau)]$ is the free particle action functional. and

$$\tilde{r}_{12} = \frac{1}{\hbar\beta} \int_0^{\hbar\beta} d\tau \, |\vec{q}_1(\tau) - \vec{q}_2(\tau)| \quad .$$ (4.3)

The effective centroid pair potential $v_{eff}(r_{c,ij})$, which is a central force and a function of temperature as well as mass, can be calculated accurately by the direct PIMC sampling methods discussed in Sec. II and saved on a one-dimensional grid. The centroid MD equations [Eq. (1.3)] can then be integrated using the centroid force computed from the pairwise centroid pseudopotential. Obviously. this scheme will be most effective for nearly classical systems where many-body quantum correlations are negligible. or for weakly interacting systems where there is a low probability for three particles to be mutually within the some relevant interaction range. For highly condensed phases of strongly quantized particles. the compact structure insures that there will be several neighbors for each quantum particle and thus the contribution from many-body quantum correlations becomes significant. In such cases. one of the more rigorous centroid MD algorithms described in the previous two sections will be necessary.

In passing. we note that three-body centroid correlations (or "dispersion") might be incorporated by fitting the excess centroid free energy due to the three-body interaction to

26

some functional form having a few adjustable parameters. This procedure *is analogous to* the determination of pseudopotentials from *ab initio* quantum chemistry calculations.

V. NUMERICAL RESULTS

In this section, the accuracy and efficiency of the various centroid MD algorithms is examined for both prototype low-dimensional models and more realistic many-body systems. Due to limitations in the available computational resources, not every model has been studied with every algorithm. Nevertheless, the numerical studies below clearly illustrate the major strengths and weaknesses of each approach. Applications of centroid MD to actual physical systems will be the subject of future publications.

The numerical examples and associated discussion are presented in the order that the algorithms appear in the previous sections. All of the algorithms are essentially the same in the numerical MD propagation of the centroid variable(s), except for the way in which the centroid force is calculated. As specified by the centroid MD algorithm, [1,3,4] the initial centroid positions were generated by Metropolis importance sampling from the centroid distribution, while the initial momenta were directly sampled from the Gaussian centroid momentum distribution. In most cases, the centroid correlation functions were plotted along with the exact Kubo transformed correlation function, [16] if available. If required, the Fourier relation in Eq. (1.1) can be used to convert the centroid correlation functions to the usual ones. [3]

A. Normal Mode Path Integral Molecular Dynamics

In order to test of the convergence of the algorithms on a simple model for which exact quantum dynamics can be obtained, the same one-dimensional anharmonic potential has been studied as in Paper II. This potential is given by

$$V(q) = \frac{1}{2}q^2 + cq^3 + gq^4 \tag{5.1}$$

27

with the parameters $c = 0.10$, $g = 0.01$, $\hbar = 1.0$, and $m = 1.0$. In these units, the inverse temperature β is given in terms of the dimensionless parameter $\beta\hbar\omega$. The potential has a single minimum at $q = 0$, exhibiting a cubic anharmonicity for small deviations from the minimum and a quartic anharmonicity for larger deviations from the minimum. At low temperatures where mode quantization effects become important, the cubic anharmonicity is the dominant perturbation. The anharmonicities in Eq. (5.1) perturb the energy gap between the ground and first excited vibrational state downward by 6% from the harmonic limit. This corresponds to a large anharmonicity for a typical molecular vibration. The temperature employed in the calculations is $\beta = 5$ which is typical of a $C-C$ single bond at 300 K. For this one-dimensional model, the exact results were obtained by first diagonalizing the nonlinear Hamiltonian in a harmonic oscillator basis set to find its eigenvalues and eigenvectors. Then, one hundred eigenstates were employed to calculate the exact Kubo-transformed time correlation functions. [3]

In the first case, the centroid force was calculated by normal mode path integral MD averaging at each time step. As discussed in Sec. II, the fictitious masses of all $P - 1$ normal modes except the centroid mode were chosen to be $m_n = m'/\beta\lambda_n^2$, where $m' = \beta$, so that the normal modes all oscillate with unit frequency. Nose-Hoover chains consisting of two thermostats with fictitious masses of 1.0 and a fictitious temperature of 1.0 were attached to each path integral normal mode. [24] The multiple time step method [29] allowed the integration of the motion due to the residue potential $\Delta V(q)$ for every 10 steps of linear motion of the reference harmonic path integral normal modes. The centroid motion was integrated in terms of the normal modes using the velocity Verlet algorithm with a time step of 0.05. The Nose-Hoover chain dynamics were calculated for 10^4 steps with a time-step of 0.005, and the centroid force [Eq. (2.1)], as well as the centroid curvature [Eq. (2.18)] and force fluctuations [Eq. (2.24)], were accumulated during the simulation. For the position correlation function of the prototype model in Eq. (5.1), the dynamics of 10^4 centroid trajectories were averaged unless otherwise specified. To speed up the convergence of the centroid force, the frequency of the harmonic reference potential was constantly updated

according to Eq. (2.16). Moreover, since the force changes smoothly with the centroid motion, the centroid force could be evaluated via the gradient correction in Eqs. (2.17) and (2.18) if the change were within some tolerance. By setting this tolerance to 20%—beyond which a new NMPIMD calculation of the centroid force was initiated—the speed of the centroid MD integration could be increased by a factor of two to three. The use of a smaller fictitious mass in the spirit of an extended Lagrangian simulation was not implemented in the present work, but such an approach has been explored recently with good success by Martyna for centroid MD. [26]

In Fig. 1, the centroid position correlation function is shown for the nonlinear oscillator of Eq. (5.1) at $\beta = 5$. The solid circles are the exact quantum results, the solid line is the NMPIMD result for the discretization parameter of $P = 20$, the dashed line is the NMPIMD result for $P = 10$, and the dot-dashed line is the result from the effective harmonic approximation for the centroid force. [3] The improvement due to the increased value of P is evident, and the brute force NMPIMD calculation is superior to the effective harmonic approximation. However, the computation time increases substantially with increasing P. Obviously, calculating the centroid force exactly using NMPIMD at each time step provides the most accurate dynamical result, but the method as presently applied will become time consuming for many-body systems having a large number of beads. (The NMPIMD calculations in Fig. 1 took approximately 50 CPU hours on an IBM RISC/6000 Model 370 workstation.)

As an aside, we note that the results shown in Fig. 1 provide further evidence that centroid MD is a method valid for *general* nonlinear potentials and *is not* intrinsically "wedded" to the effective harmonic perspective. (The latter perspective simply helps to justify centroid MD. [1,3]) The results in Fig. 1 show that a centroid MD calculation will be more accurate when the centroid force is computed *exactly*, as opposed to when it is approximated by the effective harmonic expression. The analytical justification of centroid MD for general systems is, of course, the subject of the companion paper. [4]

B. Staging Path Integral Monte Carlo

As discussed in Sec. IIB, another strategy for computing the centroid force in centroid MD is the the staging path integral MC method. The specific staging algorithm introduces a stochastic dynamics. which in the limit of $N_{MC} \rightarrow \infty$ [cf. Sec. IIB] gives exactly the centroid force and centroid MD. To test the efficiency and convergence of this method. the centroid position correlation function for the potential in Eq. (5.1) was calculated at $\beta = 5.0$ as in Fig. 1. A harmonic reference propagator of frequency $\omega = 1.0$ and $P = 10$ was used in the staging path integral MC with the number of trial chain quasiparticles in the staging algorithm adjusted to yield an acceptance rate of 50%. The staging centroid MD calculations converged to a degree comparable to that shown in Fig. 1 for a value of $N_{MC} = 10$. taking only a few CPU minutes on the IBM workstation. This calculation is therefore considerably faster than the one performed with NMPIMD. Since the staging PIMC method approximates the centroid MD asymptotically, the averaging of the centroid force is much less demanding. In addition. the normal mode transformation in the NMPIMD algorithm, which consumes a large portion of CPU time for a large value of P, is completely avoided in the staging PIMC method for centroid MD as described in Sec. IIB.

The above result strongly suggests the feasibility of using centroid MD to simulate the dynamical time correlation functions of quantum particles in many-dimensional systems As a test case. the self-diffusion process of a quantum particle in a classical solvent was studied. The solvent in this case was a Lennard-Jones fluid with the parameters $\sigma = 2.556$ Å. $\epsilon = 10.22$ K. and the solute-solvent pair potential had the simple form [30] $v(r) = [B/(C + r^6) - 1](A/r^4)$, where $A = 0.665$. $B = 89099$, $C = 12608$ (in atomic units). The simulation consisted of 512 total particles at a temperature $T = 309$ K and a reduced density of $\rho^* = 0.3$. The solute was assumed to be a quantum particle having the electron mass m_e, but Planck's constant $\hbar$ was reduced by a factor of 10 so that a discretization number of $P = 100$ was adequate in the simulation. The dynamics of 200 centroid MD trajectories were calculated for 150 time steps with an increment of 0.01 with $N_{MC} = 10$

in the staging/centroid MD algorithm. All of the data was scaled by the Lennard-Jones potential width σ, depth ϵ, and the electron mass m_e. The mean-squared displacement of the quantum solute is plotted in Fig. 2 for the centroid MD with staging PIMC method (solid line) and for classical MD (dashed line). The quantum effect is clearly manifested. though the quantum solute is far from localized [30,36]. This calculation took approximately one day of dedicated CPU time on the IBM RISC/6000 Model 370 workstation.

Though quite promising, the staging/centroid MD results are certainly preliminary. Longer computer runs and better statistics are required to evaluate diffusion constants to a acceptable degree of accuracy. Furthermore, to simulate an actual solvated electron will require a value of $P = 1000$ to converge the quantum effects. Nevertheless, this example demonstrates it is possible to carry out centroid MD calculations for realistic physical systems using the "brute force" algorithm based on staging PIMC.

C. Effective Harmonic Method: Extended Lagrangian Approach

The effective harmonic method for centroid MD [cf. Sec. IIIA] can be implemented with the extended Lagrangian approach of Sec. IIIB. This approach will produce centroid MD if the fictitious mass is sufficiently small so that the fictitious variable. namely the Gaussian width factors C_c in the present case. rapidly average the dynamics about the minimized centroid potential surface. As a test of this approach, the nonlinear potential in Eq. (5.1) was studied to determine the dependence of the extended Lagrangian method on the fictitious mass m_ξ and the time-step Δt. In Fig. 3, a single centroid trajectory is plotted for $m_\xi = 0.1$ and $\Delta t = 0.01$. Shown is the total energy (dot-dashed line), the centroid kinetic energy (solid line) and the fictitious kinetic energy *on an enlarged scale* by a factor of 10^3 (dotted line). Clearly. under the chosen conditions. the fictitious dynamics have little effect on centroid dynamics except to generate the centroid mean force. For this study, stable results were obtained until the values $m_\xi = 0.5$ and $\Delta t = 0.1$ were used. The "rule of thumb" is to choose m_ξ small enough so that the fictitious kinetic energy is less than one

31

percent of the total energy and to make Δt small enough so that the total energy does not drift more than a few percent at the end of a single trajectory. Although not shown here. the centroid position correlation function calculated with the extended Lagrangian method was found to be the same as the effective harmonic result shown in Fig. 1 (the latter result was obtained by representing the effective harmonic centroid potential on a one-dimensional grid). Since for this example (and the following one) the Gaussian averages can be expressed in closed form. the extended Lagrangian calculation takes very little CPU time. Thus. the numerical effort implicit in this method is negligible compared to either of the direct (brute force) path integral centroid MD methods.

As a more challenging test. the effective harmonic theory with the extended Lagrangian algorithm was applied to a three-dimensional particle in a non-separable potential well. given by

$$V(q_1, q_2, q_3) \; = \; \frac{1}{2} \sum_{i=1}^{3} (q_i^2 \, + \, g q_i^4) \; + \; c \, q_1 q_2 q_3 \tag{5.2}$$

with the parameters $g = 0.1$, $\hbar = 1.0$. $m = 1.0$. and $\beta = 5.0$. The extended Lagrangian centroid dynamics were carried out for the three centroid variables and the six dynamical elements of the Gaussian width factor matrix with a time step of $\Delta t = 0.01$ and a fictitious mass of $m_f = 0.1$. The quantum position correlation function (not the centroid correlation function) is shown in Fig. 4 for $c = 0.1$ along with the classical MD result. The extended Lagrangian simulation for this example was both stable and efficient. and the quantum effects are seen to be significant.

D. Effective Harmonic Method: Iterative Approach

The method is rather straightforward and was the original algorithm used in the previous calculations published in Papers II and III. In fact. the iteration method works extremely well for the examples discussed in the previous subsection (i.e.. even better than the extended Lagrangian) and will not be reproduced here. Instead. the focus will shift to a more realistic many-body system.

As has been pointed out in Sec. IIIB. the most serious potential difficulty associated with solving the transcendental equations in Eqs. (3.1)−(3.3) in many-dimensional space is the evaluation of the Gaussian averages. Several approaches were proposed and formulated in Sec. III. For the present purposes. the Gaussian representation of pair potentials in Eq. (3.17) is the most convenient and efficient. A set of five of Gaussian parameters was found to be accurate in representing a Lennard-Jones pair potential. [37] In order to demonstrate the validity of the effective harmonic approximation and the Gaussian representation of the Lennard-Jones potential, in Fig. 5 the centroid force thus calculated is plotted (solid line) along with the results of an exact PIMC calculation (solid circles). The parameters were taken to be $\beta = 1.0$. $m = 1.0$. and $\hbar = 0.1$. so the PIMC calculations were performed for $P = 20$ with 10^3 MC passes. The results are in remarkably good agreement.

Next the effective harmonic theory with the iterative algorithm for the centroid force was applied to study a quantum particle solvated in a pairwise Lennard-Jones classical fluid similar to that described in Sec. VB. The Lennard-Jones interaction between the quantum particle and the solvent particles was also represented by five independent Gaussian functions. The well depth and width of Lennard-Jones potential were taken as the natural units. and a unit mass was assumed for both the solvent and the solute. A total of 125 solvent particles in a periodic cubic were used to model the solvent at a reduced density 0.8 and at a reduced temperature 1.0 The quantum nature of the solute particle was adjusted by varying the Planck's constant $\hbar$ from $\hbar = 0.0$ to $\hbar = 0.3$ in the reduced units. The dynamics of 10^3 independent centroid trajectories were then integrated for 500 time steps of duration 0.01. At the initial stage of the centroid MD simulation. $10 - 20$ iterations were needed for convergence in computing the centroid force at each time step. After the centroid began to move. the self-consistent parameter set from the previous time step was taken as the input to the iterations at the current time step and. accordingly, only $1 - 3$ iterations were needed to converge the centroid force.

The mean square displacement of the solute is plotted in Fig. 6 for centroid MD (solid line) and for classical MD (dashed line). The diffusion constant measured from the slope

33

of the displacement curve shows a 20% decrease due to quantum effect in this case. The effective harmonic centroid MD method with the iterative approach was found to be stable and highly efficient. The results in Fig. 6 were obtained in several hours of CPU time on the IBM RISC/6000 Model 370 workstation.

E. Centroid Pseudopotential Method

First of all, it is important to examine the suggestion in Sec. IV that an effective pairwise centroid potential can capture the dominant quantum effects in the many-body centroid potential surface. Since only the force is relevant to centroid MD, the following results will be expressed in terms of the centroid force instead of the centroid potential. For convenience, a Lennard-Jones potential was employed with the reduced parameters $\sigma = 1.0$, $\epsilon = 1.0$, $m = 1.0$, $\beta = 1.0$, and $\hbar = 1.0$. The computational procedure is described as follows:

(1) The centroid force between a pair of quantum particles interacting via the Lennard Jones potential was calculated as a function of separation between their centroids in a PIMC simulation.

(2) The total centroid force between the three particles arranged on an equilateral triangle was then calculated in a similar fashion by uniformly changing the distance of the three sides of the triangle.

(3) The pairwise pseudopotential method was then applied to the same three-particle system with the pair potential obtained from step (1).

The results from the direct simulation in step (2) and the pseudopotential approximation in step (3) are plotted in Fig. 7 and agree quite well except at very close (and improbable) distances.

In paper II, the self-diffusion process in fluid neon [38] was studied with centroid MD by including the leading correction in the pair centroid potential. The same calculation has been carried out here using the pseudopotential method. The parameters of the system and details of the centroid MD simulation can be found in Paper II (cf. Sec. IV C and Table I

in that paper). To illustrate the difference between the two approximations, in Fig. 8 the pair centroid pseudopotential force used in this calculation is plotted (solid line) against the approximate centroid force used in the Paper II (dot-dashed line) and the classical Lennard-Jones force (dashed line). Then, in Fig. 9 the centroid velocity time correlation function is plotted for quantum neon (solid line) using the pseudopotential method and for classical neon (dashed line). Evidently, the more repulsive centroid force shown in Fig. 8 leads to the decrease in the quantum diffusion constant seen in Fig. 9 (i.e., through the integral of the centroid velocity autocorrelation function in the Green-Kubo formula for the diffusion constant [3]).

VI. CONCLUDING REMARKS

This paper is solely devoted to the development of numerical algorithms for centroid MD and, in turn, it sets the stage for a broad spectrum of applications. Though centroid MD makes the study of quantum dynamics in many-body systems a possibility, the numerical integration of the centroid MD equations is by no means trivial. This is because the centroid force $\vec{F}_c(\vec{q}_c)$ in Eq. (1.4) is a quantum mean force which cannot be evaluated exactly by simple analytical expressions. Therefore, several algorithms for centroid MD have been outlined and tested in the present paper. Though these algorithms have been described in considerable detail, some remarks are in order regarding the outlook for their application in realistic simulations.

Strictly speaking, the quantum imaginary time path fluctuations about the centroid variable must be completely averaged in order to compute the centroid force in Eq.(1.4) at each time step in the centroid MD integration. The NMPIMD/centroid MD algorithm in Sec. IIA will essentially produce the exact centroid force at each time step, but the preliminary results reported in Sec. VA suggest its application to a real many-body system will be formidable in any practical sense. Perhaps a more complete examination of the extended Lagrangian aspects of the NMPIMD algorithm will provide a more optimistic prognosis for

the method. [26] On the other hand, the results from the staging PIMC/centroid MD algorithm developed in Sec. IIB suggest that a brute force centroid MD calculation is indeed within the realm of possibility for realistic systems. The staging PIMC/centroid MD scheme is simpler and faster than NMPIMD/centroid MD algorithm. The preliminary results suggest that a single quantum particle immersed in a classical solvent with $P = 100 - 1000$, or an ensemble of quantum particles, each with $P \approx 20 - 30$, can be treated with the staging PIMC/centroid MD algorithm on a higher-end computer workstation. Of course, computer performance is rapidly increasing, so optimism is clearly in order. Moreover, the outlook for implementing centroid MD on a massively parallel computer seems most promising, though such algorithms remain to be explored.

For systems which are presently beyond the reach of the brute force path integral centroid MD methods, the effective harmonic centroid MD algorithm of Sec. III is an attractive option. In fact, this algorithm will always provide a highly efficient alternative to the brute force methods in systems where the quantum modes are predominantly influenced by positive curvature in the potential (i.e., so that the minimization of the effective harmonic potential is efficient). The vibrational dynamics and relaxation of condensed phase polyatomic molecules, or perhaps the dynamics of quantum clusters, may be ideal candidates for the effective harmonic algorithm.

Due to its simplicity and flexibility, the centroid pseudopotential method described in Sec. IV is particularly attractive for very large systems, provided those systems are not too quantum in nature or have low densities. For example, the transport coefficients of nearly classical fluids, simulations of quantum friction, and calculations of quantum solvent spectra could all be investigated with this method (and probably with the others as well—at least in time).

As a final point, we note that the algorithms described in the present paper might be *combined* to greatly enhance the capability of centroid MD for the study of real systems. Consider the example of proton exchange dynamics between two solutes in a quantized solvent such as water. The proton centroid dynamics might be treated by one of the brute

force path integral methods. the solute intramolecular centroids could be integrated through the effective harmonic approach. while the solvent-solute and solvent-solvent interactions could be approximated by the centroid pseudopotential method. The feasibility of such an algorithm is insured by the so-called free energy Born-Oppenheimer approximation. [19] A variety of applications of centroid MD will be reported in future publications.

ACKNOWLEDGMENTS

APPENDIX A: EVALUATION OF THE SUBMATRIX C'_C IN EQ. (3.13)

In general, the centroid-constrained correlation function in Eq. (3.3) and Eq. (3.5) is a $(3N \times 3N)$-th order matrix for an N-body system in three dimensional space. For the simplicity of notation, the three space indices will be eliminated here. Thereby, for a particle with three spatial components the matrix C_c is re-defined below as an N-th order matrix, with each element understood to be defined as

$$C_{c,ij} \equiv \begin{pmatrix} C_{c,ij}^{11} & C_{c,ij}^{12} & C_{c,ij}^{13} \\ C_{c,ij}^{21} & C_{c,ij}^{22} & C_{c,ij}^{23} \\ C_{c,ij}^{31} & C_{c,ij}^{32} & C_{c,ij}^{33} \end{pmatrix} \quad . \tag{A1}$$

Here, the subscripts denote the particle index and the superscripts denote the three spatial dimensions. It is also to be noted that all elements of this matrix depend on the centroid variables of the N-body system. One can now partition the inverse of the matrix C_c, defined as B, such that

$$C_c^{-1} = B = \begin{pmatrix} b_{11} & b_{12} \\ b_{21} & b_{22} \end{pmatrix} \quad . \tag{A2}$$

Here, $b_{11} = B_{11}$ is treated as a matrix element [which is, according to Eq. (A1), actually a matrix of order 3]. $b_{12} = (B_{12}, B_{13}, \cdots, B_{1N})$ is like a row vector, b_{21} is like a column vector such that $b_{21} = b_{12}^t$, and b_{22} is like an $(N-1) \times (N-1)$-th order matrix.

With the above notation in hand, all of the other variables $\{q_2, \ldots, q_N\}$ in Eq. (3.8) can be integrated out to give a reduced Gaussian average [cf. Eq. (3.12)], with the reduced Gaussian distribution given by

$$\begin{aligned} P(q_1) &= \frac{\prod_{i=2}^{N} \int dq_i \, exp\left(-\vec{q} \cdot B \cdot \vec{q}/2\right)}{\int d\vec{q} \, exp\left(-\vec{q} \cdot B \cdot \vec{q}/2\right)} \\ &= \left[\frac{det(2\pi b_{22}^{-1})}{det(2\pi B^{-1})} \right] exp\left[-q_1(b_{11} - b_{12}b_{22}^{-1}b_{21})q_1/2\right] \quad . \end{aligned} \tag{A3}$$

On the other hand, one has the matrix element from Eq. (A1), i.e.,

$$C_{c,11} = (B^{-1})_{11} = det(b_{22})/det(B) \tag{A4}$$

38

where the denominator. after some algebra. can be written as

$$\det(\mathbf{B}) \;=\; (b_{11} - \mathbf{b}_{12}\mathbf{b}_{22}^{-1}\mathbf{b}_{21}) \det(\mathbf{b}_{22}) \quad . \tag{A5}$$

Therefore. the reduced matrix $\mathbf{C}_c' \equiv \mathbf{C}_{c,11}$ can be introduced so that the reduced Gaussian distribution in Eq. (A3) reads as

$$P(q_1) \;=\; \frac{1}{\det(2\pi\mathbf{C}_c'^{-1})} \, exp\left(- q_1 \cdot \mathbf{C}_c' \cdot q_1/2\right) \quad . \tag{A6}$$

where according to the notation used here $\mathbf{C}_c'$ is a matrix of order 3 and q_1 is a three-dimensional vector.

As stated in the main text. a pair potential only depends on the relative position of the pair particles. Therefore. the preceding result should be expressed in terms of $\vec{r}_{ij} = \vec{q}_i - \vec{q}_j$, the vector connecting particles i and j. Thereby, an uniform transformation is required to obtain the relevant matrix element, i.e..

$$\mathbf{C}_{c,ij}'^{-1}(\vec{q}_c) \;=\; \frac{\mathbf{C}_{c,ii}^{-1} - 2\mathbf{C}_{c,ij}^{-1} + \mathbf{C}_{c,jj}^{-1}}{4} \tag{A7}$$

which defines the reduced Gaussian distribution for the variable $\vec{r}_{ij}$ in Eqs. (3.11) and (3.12).

REFERENCES

[1] J. Cao and G. A. Voth, J. Chem. Phys. **99**, 10070 (1993).

[2] J. Cao and G. A. Voth, J. Chem. Phys. **100**, xxxx (1994).

[3] J. Cao and G. A. Voth, J. Chem. Phys. **100**, xxxx (1994).

[4] J. Cao and G. A. Voth, J. Chem. Phys. **xx**, xxxx (1994).

[5] See Ref. [6], pp. 279-286.

[6] R. P. Feynman and A. R. Hibbs, *Quantum Mechanics and Path Integrals* (McGraw-Hill Book Company, New York, 1965).

[7] R. P. Feynman, *Statistical Mechanics* (Addison-Wesley, MA, 1972), chap. 3.

[8] L. S. Schulman, *Techniques and Applications of Path Integration* (John Wiley and Sons, Inc., New York, 1986).

[9] M. S. Swanson, *Path Integrals and Quantum Processes* (Academic Press, San Diego, 1992).

[10] D. Chandler, in *Liquides, Cristallisation et Transition Vitreuse Les Houches, Session LI*, edited by D. Levesque, J. Hansen, and J. Zinn-Justin (Elsevier, New York, 1991).

[11] B. J. Berne and D. Thirumalai, Annu. Rev. Phys. Chem. **37**, 401 (1986).

[12] J. D. Doll, D. L. Freeman, and T. L. Beck, Adv. Chem. Phys. **78**, 61 (1990).

[13] R. P. Feynman and H. Kleinert, Phys. Rev. A. **34**, 5080 (1986).

[14] R. Giachetti and V. Tognetti, Phys. Rev. Lett. **55**, 912 (1985).

[15] J. Cao and B. J. Berne, J. Chem. Phys. **92**, 7531 (1990).

[16] R. Kubo, N. Toda, and N. Hashitsume, *Statistical Physics II* (Springer-Verlag, Berlin, 1985).

[17] For reviews of numerical and analytical path integral methods, see Refs. [10–12].

[18] J. D. Doll and J. E. Gubernatis, *Quantum Simulations of Condensed Matter Phenomena* (World Scientific, Singapore, 1990).

[19] J. Cao and B. J. Berne, J. Chem. Phys. **99**, 2902 (1993).

[20] E. L. Pollock and D. M. Ceperley, Phys. Rev. B **30**, 2555 (1984).

[21] M. Sprik, M. L. Klein, and D. Chandler, Phys. Rev. B **31**, 4234 (1985).

[22] M. Parrinello and A. Rahman, J. Chem. Phys. **80**, 860 (1984).

[23] R. D. Coalson, D. L. Freeman, and J. D. Doll, J. Chem. Phys. **85**, 4567 (1986).

[24] G. J. Martyna, M. Tuckerman, and B. J. Berne, J. Chem. Phys. **98**, 1990 (1992).

[25] M. Tuckerman, B. J. Berne, G. J. Martyna, and M. L. Klein, J. Chem. Phys. **99**, 2796 (1993).

[26] G. J. Martyna, (to be submitted, 1994). This author also suggests using the extended Lagrangian approach to calculate centroid MD trajectories.

[27] R. Car and M. Parrinello, Phys. Rev. Lett. **55**, 2471 (1985).

[28] D. K. Remler and P. A. Madden, Mol. Phys. **70**, 921 (1990), this reference contains a good review and discussion of the Car-Parrinello extended Lagrangian technique for first-principles molecular dynamics simulations.

[29] M. Tuckerman, G. J. Martyna, and B. J. Berne, J. Chem. Phys. **97**, 1990 (1992).

[30] D. F. Coker, B. J. Berne, and D. Thirumalai, J. Chem. Phys. **86**, 5689 (1987).

[31] B. J. Berne and R. Pecora, *Dynamic Light Scattering* (Wiley-Interscience, New York, 1976).

[32] G. A. Voth, Phys. Rev. A **44**, 5302 (1991).

[33] See Ref. [6], pp. 303-307, and Ref. [7], pp. 86-96.

[34] J. Cao and B. J. Berne, J. Chem. Phys. **97**, 8628 (1992).

[35] M. J. Thompson, K. S. Schweizer, and D. Chandler, J. Chem. Phys. **76**, 1128 (1982).

[36] D. Chandler, Y. Singh, and D. M. Richardson, J. Chem. Phys. **81**, 1975 (1984).

[37] G. J. Martyna, (private communication).

[38] D. Thirumalai, R. W. Hall, and B. J. Berne, J. Chem. Phys. **81**, 2523 (1984).

FIGURES

FIG. 1. A plot of the centroid position correlation function for the nonlinear oscillator of Eq. (5.1) at $\beta = 5$. The solid circles are the exact quantum results, the solid line is the NMPIMD result for $P = 20$, the dashed line is the NMPIMD result for $P = 10$, and the dot-dashed line is the result of the effective harmonic approximation for the centroid force (see Paper II)

FIG. 2. A plot of the mean square displacement for a quantum particle solvated in a classical neon fluid. The solid line is the stochastic centroid MD with staging PIMC described in Sec. IIB while the dashed line is for classical MD.

FIG. 3. A plot of the energy data for a single trajectory for the potential in Eq. (5.1) as calculated with the extended Lagrangian centroid MD method of Sec. IIIB. The dot-dashed line is the total energy, the solid line is the centroid kinetic energy, and the dashed line is the fictitious kinetic energy enlarged by a factor of 10^3.

FIG. 4. A plot of the real time position correlation function calculated by the extended Lagrangian centroid MD method of Sec. IIIB for the three-dimensional potential given in Eq. (5.2) at a temperature of $\beta = 5$. Also shown is the classical MD result.

FIG. 5. A plot of the centroid force for a Lennard-Jones potential. The solid circles represent exact results from a PIMC simulation, while the solid line represents the effective harmonic approximation from Eqs. (3.1)−(3.3) with the Gaussian representation of the Lennard-Jones potential in Eq. (3.17).

FIG. 6. A plot of the mean squared displacement of a quantum Lennard-Jones particle solvated in a classical Lennard-Jones fluid. The solid line is the centroid MD result obtained with the effective harmonic centroid force solved iteratively (cf. Sec. IIIC), while the dashed line is the classical MD result.

FIG. 7. A plot of the total centroid force between three Lennard-Jones particles distributed on a equilateral triangle. The solid circles are the exact PIMC simulation results. while the solid line is the pseudopotential approximation of Sec. IV.

FIG. 8. A plot of the pair force between two Lennard-Jones particles as a function of separation. The solid line is exact pair centroid force used in the pseudopotential calculation. the dot-dashed line is the approximate pair centroid force used in Paper II. and the dashed line is the classical Lennard-Jones force.

FIG. 9. A plot of the centroid velocity autocorrelation function for fluid neon. The solid line is the centroid MD result calculated with the centroid pseudopotential approximation. while the dashed line is the classical MD result.
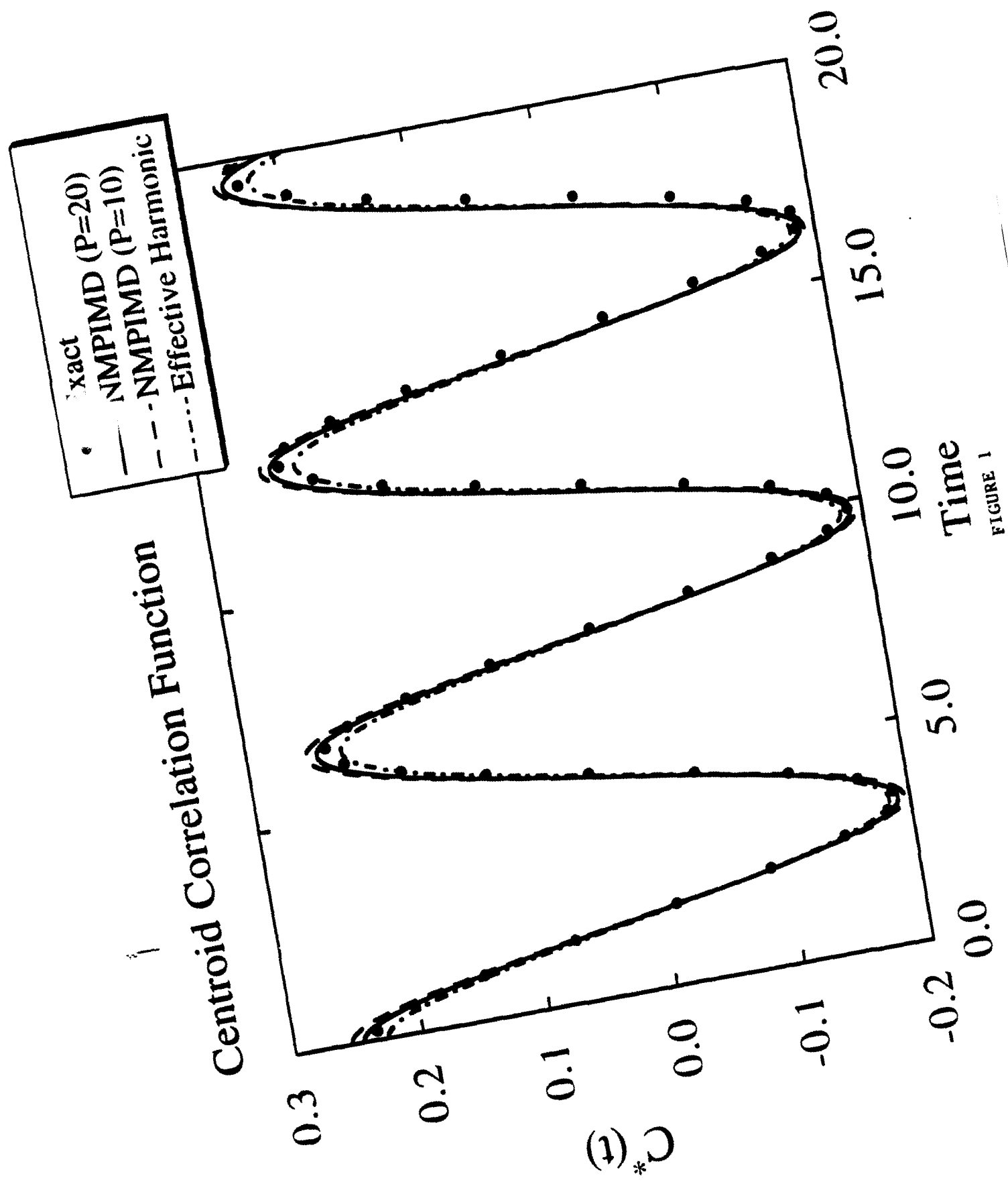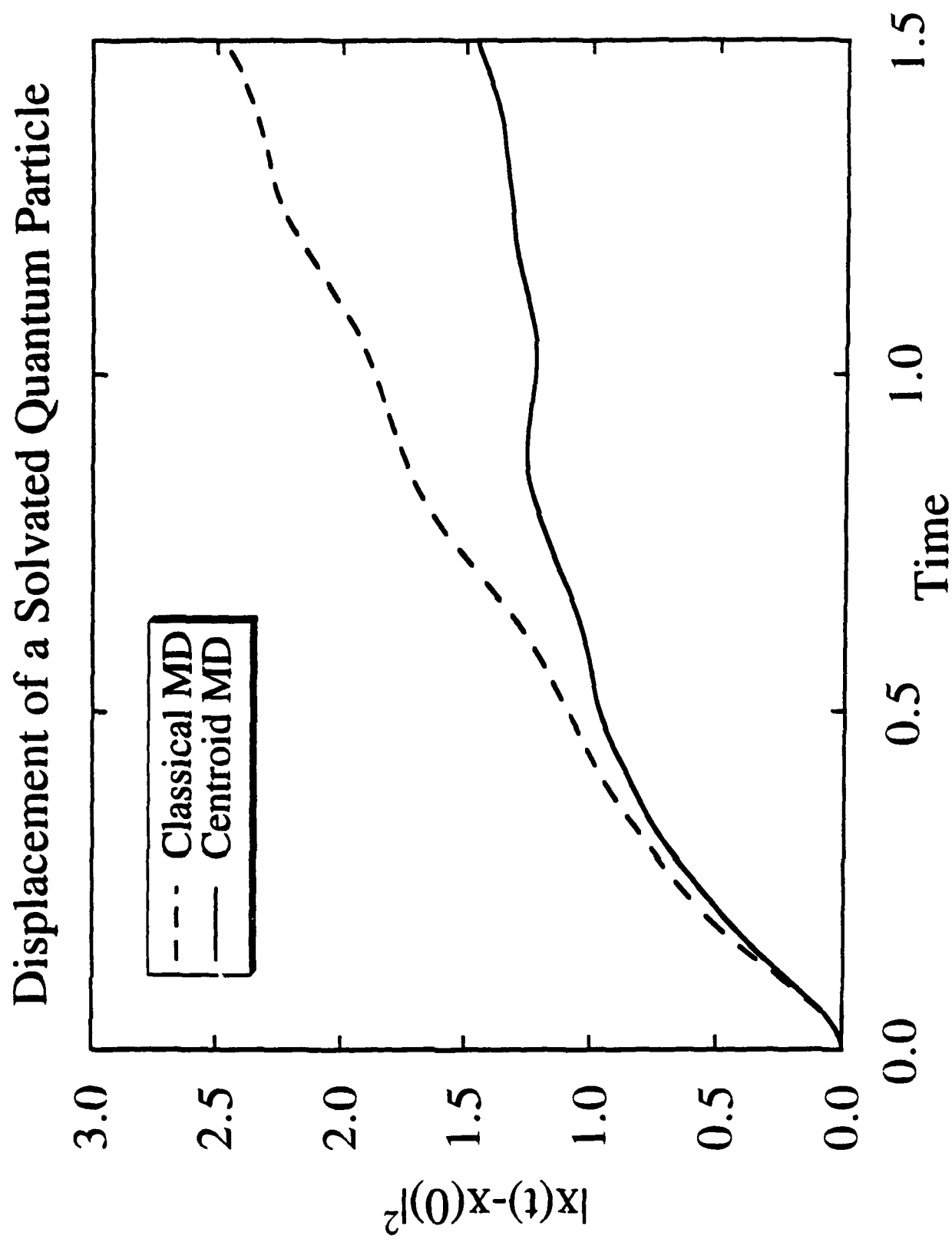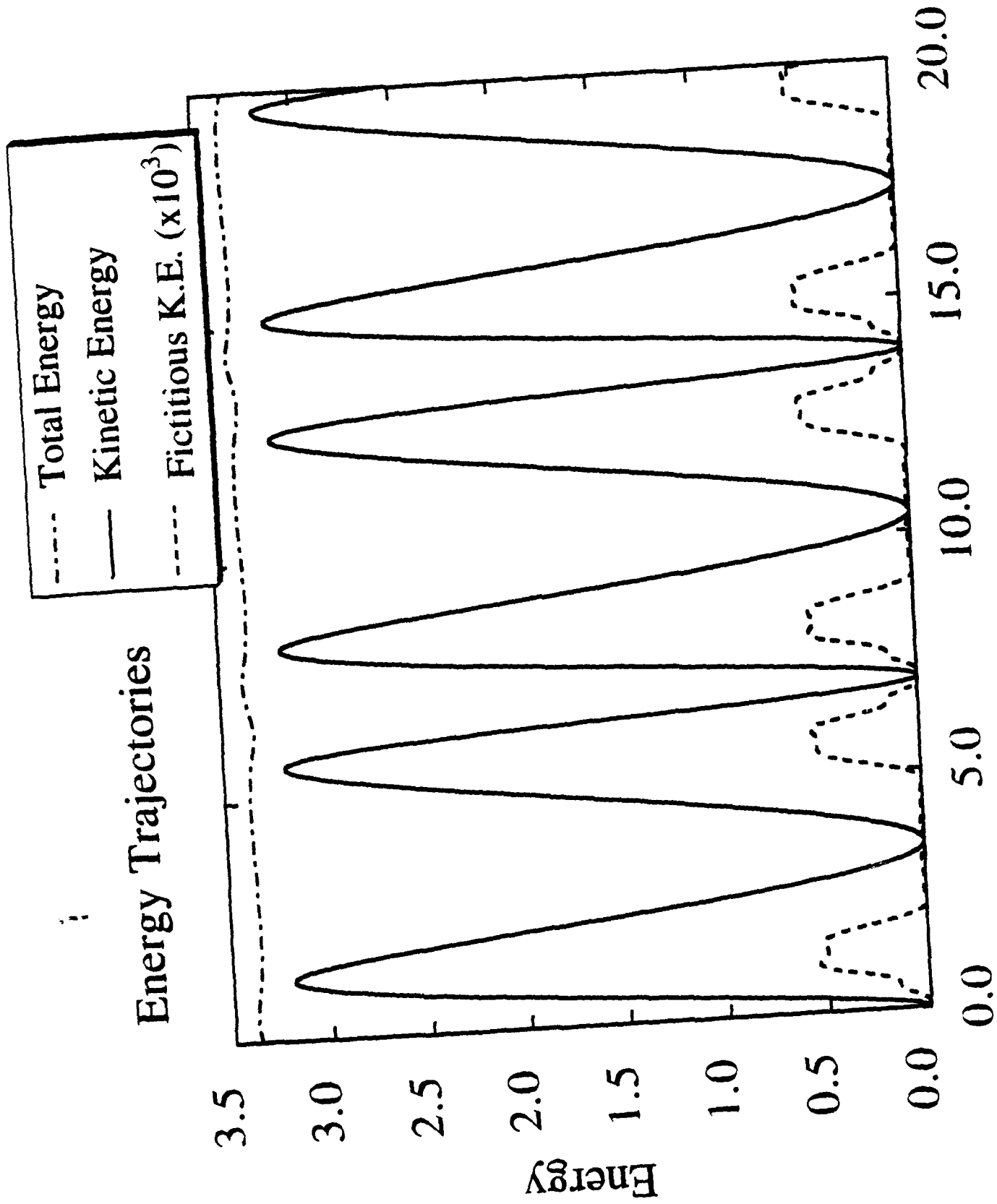
Centroid Correlation Function

FIGURE 1

Legend:
- Exact
- NMPIMD (P=20)
- NMPIMD (P=10)
- Effective Harmonic

Axes: $C^*(t)$ vs Time

Y-axis values: 0.3, 0.2, 0.1, 0.0, -0.1, -0.2

X-axis values: 0.0, 5.0, 10.0, 15.0, 20.0

Displacement of a Solvated Quantum Particle

- - - Classical MD
—— Centroid MD

$|x(t)-x(0)|^2$

Time

FIGURE 2

Energy Trajectories

Total Energy
Kinetic Energy
Fictitious K.E. (x10^3)

Energy

Time

0.0   5.0   10.0   15.0   20.0

FIGURE 3

The Position Correlation Function

FIGURE 4

Centroid Force

- Exact (PIMC)
— Effective Harmonic Approx.

$F_c(r)$

FIGURE 5

Displacement of a Solvated Quantum Particle

Classical MD
Centroid MD

$|x(t)-x(0)|^2$

Time

FIGURE 6

Centroid Force

Exact (PIMC) ●
Pseudopotential ——

$F_c(r)$

r

FIGURE 7

Centroid Pair Force

FIGURE 8

Velocity Autocorrelation Function

Classical MD
Centroid MD

$C_{vv}(t)$

Time

FIGURE 9